Catalysis Today 150 (2010) 42–48

Contents lists available at ScienceDirect

Catalysis Today

journal homepage: www.elsevier.com/locate/cattod

Influence of the porous structure of activated carbons in the activity of ATRP catalyst for methyl methacrylate polymerization

S. Barrientos-Ramírez [a,b], G. Montes de Oca-Ramírez [a], A. Sepúlveda-Escribano [a,*], M.M. Pastor-Blas [a], A. González-Montiel [b], F. Rodríguez-Reinoso [a]

[a] Department of Inorganic Chemistry, University of Alicante, P.O. Box 99, 03080 Alicante, Spain
[b] CID, Research & Technological Development Centre, Av. de los Sauces No. 87, Mz. 6, 52000 Lerma, Mexico

ARTICLE INFO

Article history:
Available online 26 November 2009

Keywords:
ATRP
Activated carbon
Porosity
Catalyst
PMMA
Controlled polymerization

ABSTRACT

Three activated carbons exhibiting different textural characteristics were considered as support for CuBr–HMTETA catalyst in the Atom Transfer Radical Polymerization (ATRP) of methyl methacrylate. The pore distribution of the activated carbons played an important role in the control of the polymerization reaction: polydispersity index always failed in the range 1.1–1.3. However, the accessibility of the catalyst to pores in the activated carbon was limited by pore size and growing polymer size. Catalyst located within the micropores of spherical carbon was isolated from the growing polymer chains during the polymerization reaction, which took place at the mesopores. Mesoporous structure of LMA F-12 carbon enhanced polymerization rate but control over the molecular weight distribution was decreased. A carbon with an adequate distribution of micro- and mesoporosity (RGC-30) provided a suitable balance between activation and deactivation processes involving $Cu^{(I)}$ and $Cu^{(II)}$ catalytic species, which resulted in the appropriate control of the molecular weight during the methyl methacrylate polymerization reaction.

1. Introduction

Many catalysts consist of metals or metal compounds supported on an appropriate support which allows to maintain the catalytically active phase in a highly dispersed state. However, it is well documented that the role of the support is not merely that of a carrier; it may actually contribute to catalytic activity and it may even react to some extent with other catalyst components during the manufacturing process. Furthermore, the interaction between the active phase and the support can affect the catalytic activity [1–3].

A catalyst is characterized by its chemical composition, surface area, stability and mechanical properties. When the active phase is spread on a support, it disperses throughout the pore system, in such a way that a large active surface is obtained. Besides, a supported catalyst facilitates the flow of gases through the reactor and the diffusion of reactants through the pores to the active phase, improving the dissipation of reaction heat, retarding the sintering of the active phase and increasing the poison resistance. The selection of the support is based on a series of desirable characteristics [4]: inertness, stability under reaction and regeneration conditions, adequate mechanical properties, appropriate physical form for the given reactor, high surface area (which is usually, but not always, desirable), porosity and suitable chemical nature. From a wide range of possible supports, in practice only three (alumina, silica and carbon - mainly activated carbon) combine these characteristics optimally [5–8].

Controlled/"living" radical polymerization using transition metals based catalysts, also known as Atom Transfer Radical Polymerization (ATRP), is a leading industrial method to produce polymers with well-defined compositions, architectures and functionalities [9–15,18–30]. Living polymerization techniques are used when the polymerization proceeds in absence of irreversible chain transfer and chain termination steps [9]. ATRP requires the design of an appropriate catalyst (transition metal compound and ligands), using an initiator with a suitable structure, and adjusting the polymerization conditions such that the molecular weights increased linearly with conversion and the polydispersities were typical of a living process. ATRP can be carried out in a homogeneous system (e.g. bulk, solution). However, a considerable amount of catalyst is necessary to obtain considerable rates of polymerization, and the removal of the catalyst once the polymerization is completed increases the economical cost of the industrial process [11].

* Corresponding author.
E-mail address: asepul@ua.es (A. Sepúlveda-Escribano).

0920-5861/$ – see front matter © 2009 Elsevier B.V. All rights reserved.
doi:10.1016/j.cattod.2009.10.015

Thus, supporting the catalyst would improve the ATRP process as the catalyst could be easily recovered and potentially recycled. Some earlier attempts with heterogeneous catalyst have been made [13–15]. However, the potential of carbon as catalyst support for ATRP systems has not yet been exploited probably because carbon materials are strong radical scavengers due the presence of polycondensed aromatic rings and quinonic and phenolic oxygens. Propagating polymeric radicals in ATRP systems can be easily trapped by carbon surface during the polymerization.

Matyjaszewski and coworkers [16] reported the functionalization of a carbon black surface with ATRP initiating sites and subsequent ATRP of n-butyl acrylate (n-BA) from the surface of carbon black. They reported a stable radical concentration in the systems, a small increase in molecular weight and a much larger decrease in the polymerization rate. This was attributed to the fact that radical trapping could not be the only reason for the decrease of polymerization rate. A substantial amount of the monomer could diffuse into the internal voids of the carbon black aggregates. Additionally some $Cu^{(I)}$ species could also be adsorbed on carbon black, reducing the ATRP rate [17].

In this study, a copper-mediated ATRP has been considered using $Cu^{(I)}Br$–[1,1,4,7,10,10-hexamethyltriethylenetetramine] (CuBr–HMTETA) as a catalyst and methyl-α-bromophenylacetate [MBP] as initiator. Activated carbon has been considered as a catalyst support for ATRP of methyl methacrylate (MMA) via an atom transfer polymerization process, and influence of carbon pore size distribution on the polymerization reaction performance has been studied. The use of activated carbons as catalyst support is expected to decrease hindering of diffusivity and minimize steric effects, being these effects influenced by carbon porosity. Therefore, the influence of the carbon porosity in the catalyst activity will be analyzed. Thus, three activated carbons with similar surface chemistry and different textural properties were analyzed. Surface functionalization of carbon and discussion on the effect of its surface chemistry will be reported later on.

2. Experimental

Three activated carbons with different textural properties were considered in this study as catalyst support: two commercial activated carbons (RGC-30 and spherical carbon), and a carbon synthesized in the Advanced Materials Laboratory, University of Alicante (LMA F-12). Textural characterization of these carbons was carried out by N_2 and CO_2 adsorption. N_2 at 77 K is commonly used for determining adsorption properties of porous materials. Although nitrogen gas can only access pores larger than about 0.4 nm, due to the low temperature of the measurement, restricted diffusion could occur even for this small pore size [31,32]. CO_2 adsorption at 273 K is useful when carbons contain very narrow microporosity (ultramicropores). This temperature is high enough to avoid diffusion problems, and the maximum relative pressure that can be reached in a conventional adsorption system is very low, $p/p_o = 0.03$. Besides, this technique does not require very complex equipment [33,34]. Therefore, it has been suggested as a complimentary technique to N_2 adsorption [35]. CO_2 adsorption isotherms are usually evaluated by Dubinin–Radushkevich (D–R) method [2,36].

2.1. Materials

To conduct the ATRP reaction, methyl methacrylate (99.9%) from Aldrich was distilled under vacuum and stored at 269 K. Toluene (99%), CuBr (99.99%), methyl-α-bromophenylacetate (MBP, 99%) and 1,1,4,7,10,10-hexamethyltriethylenetetramine (HMTETA, 99%) were also obtained from Aldrich and used without prior treatment.

Polymerization with $Cu^{(I)}Br$/HMTETA physisorbed on activated carbon was carried out as follows [37]: a typical ratio between methyl methacrylate (MMA), copper and initiator (MBP) was set: [MMA]/[Cu]/[MBP] = 100/1/1. Therefore, $Cu^{(I)}Br$ (1.35 mmol), toluene (40 ml), and activated carbon (3 g) were added to a 200 ml 4560 mini-bench top reactor (Parr Instrument Co.). HMTETA ligand (1.35 mmol) and toluene (20 ml) were added to the cylinder. Three helium purge cycles were applied to the reactor and cylinder. The HMTETA ligand solution was transferred from the cylinder to the reactor vessel and stirred overnight to support the catalyst on the activated carbon support.

MMA (135 mmol), initiator (MBP, 1.35 mmol) and toluene (25 ml) were added to the cylinder and purged under three helium purge cycles. The mixture was then added to the reactor vessel. The reactor was heated at 358 K under stirring. Kinetic samples, 1 ml, were taken out using a helium-purged sampler. The conversion was measured by ^1H NMR from the ratio between the OCH_3 signal intensity in the polymer (3.60 ppm) and the monomer (3.75 ppm). The molecular weight and the polydispersity of the polymer were measured by GPC.

2.2. Experimental techniques

2.2.1. Nuclear magnetic resonance (NMR) spectroscopy

^1H NMR spectra were recorded on a Bruker AC-300 spectrometer (Bruker BioSpin, Billerica, MA, USA) at 300 MHz. ^1H NMR chemical shifts in $CDCl_3$ were reported from 0.00 ppm using tetramethyl silane (TMS) as an internal reference.

2.2.2. Molecular weight measurements

Number- and weight-average molecular weights (M_n and M_w, respectively) were determined by gel permeation chromatography (GPC: SHK polystyrene gel column; flow rate: 1.0 ml/min) relative to polystyrene using tetrahydrofuran (THF) as solvent at 298 K with refractive index detector. Data were recorded and manipulated using the Waters Millennium software package provided with the instrument.

2.2.3. Inductively coupled plasma atomic emission spectroscopy (ICP-OES)

The ICP-OES analyses were performed on the Inductively Coupled Plasma-Optical Emission Spectrometer Perkin-Elmer Optima 3000™ (Norwalk, CT, USA). The sample was quantified with great accuracy and adequately dissolved with requisite hydrogen fluoride. Then the solution was vaporized to remove silicon fluoride. The remaining residue was dissolved by 0.2 mol/L hydrogen chloride and the solution formed was adjusted to weak acidity by ammonia. The resulting solution was diluted and was ready for ICP-OES measurement.

2.2.4. Nitrogen adsorption isotherms

Nitrogen adsorption isotherms were determined in a Coulter Omnisorb-610 equipment at 77 K. Before the experiment, the samples were outgassed at 523 K for 4 h under vacuum (10^{-6} kPa). The specific surface area (S_{BET}) was obtained using the BET method. The micropore volume (V_{mic}) was deduced from the adsorption data by means of the α-method [38]. Finally, the mesopore volume (V_{mes}) was estimated by subtracting the micropore volume (V_{mic}) from the total volume adsorbed at $p/p_o = 0.95$.

2.2.5. CO_2 adsorption isotherms

CO_2 adsorption isotherms were recorded by subatmospheric CO_2 adsorption in an Autosorb 6 (Quantachrome) apparatus at 273 K. The volume of narrow micropores of carbons was obtained by applying the D–R equation to the absorption data for CO_2 [2].

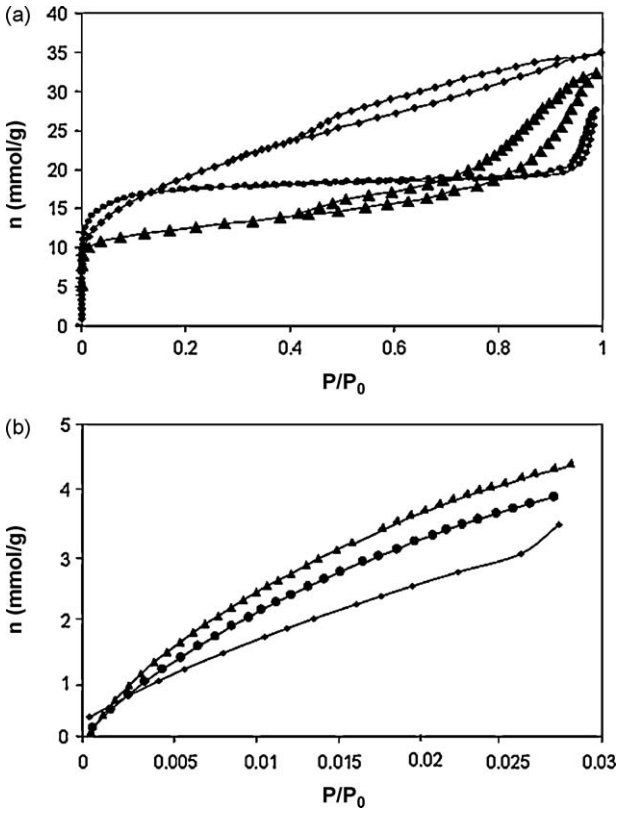

Fig. 1. Adsorption isotherms of (a) N_2 at 77 K and (b) CO_2 at 273 K; of spherical carbon (●), RGC-30 (■) and LMA F-12 (▲) activated carbons.

3. Results and discussion

3.1. Textural characterization of activated carbons

Textural properties of activated carbons used as catalyst support were determined by N_2 adsorption at 77 K (Fig. 1a) and CO_2 adsorption at 273 K (Fig. 1b). In all cases, a type I isotherm, characteristic of microporous solids in which the pore filling occurs at low relative pressures, is observed. LMA F-12 and RGC-30 carbons show isotherms with non-coincident adsorption and desorption branches. This hysteresis loop indicates capillary condensation associated to mesoporosity. Quantification of porosity in terms of specific surface (S_{BET}) and micropore volume (V_{mic}) using the BET (Brunauer–Emmet–Teller) and the D–R (Dubinin–Radushkevich) equations applied to data obtained from nitrogen adsorption isotherms is shown in Table 1. The volume of narrow microporosity (V_n) was obtained by applying the D–R equation to data obtained from CO_2 adsorption isotherms (Fig. 1b).

Taking into account the relative ratio between the micropore volume and the total volume (V_{mic}/V_t), it can be concluded that spherical carbon exhibits approximately 80% of pore volume within the micropores range ($V_{mic}/V_t = 0.80$). LMA F-12 carbon shows only 30% microporosity and RGC-30 carbon shows an intermediate range of microporosity (45% microporosity and 55% mesoporosity). This indicates a considerable narrower porosity and a higher micropore volume in spherical carbon. This is also evident from the isotherm knee at low relative pressures that is sharper for the spherical carbon, indicating the presence of narrow and uniform micropores. Therefore, three activated carbons with different textural characteristics were selected to evaluate the influence of porosity in the activity of CuBr/HMTETA catalyst: a highly microporous activated carbon (spherical), a highly mesoporous activated carbon (LMA F-12) and an activated carbon with a considerable amount of both micro- and mesopores (RGC-30).

Table 1
Specific surface areas and pore characteristics of activated carbon supports.

Activated carbon	S_{BET} ($m^2 g^{-1}$)	V_t ($m^2 g^{-1}$)	V_{meso} ($m^2 g^{-1}$)	V_{mic} ($m^2 g^{-1}$)	V_n ($m^2 g^{-1}$)	V_{mic}/V_t
RGC-30	1527	1.16	0.65	0.51	0.31	0.45
LMA F-12	670	0.87	0.61	0.26	0.30	0.30
Spherical	1195	0.60	0.12	0.48	0.40	0.80

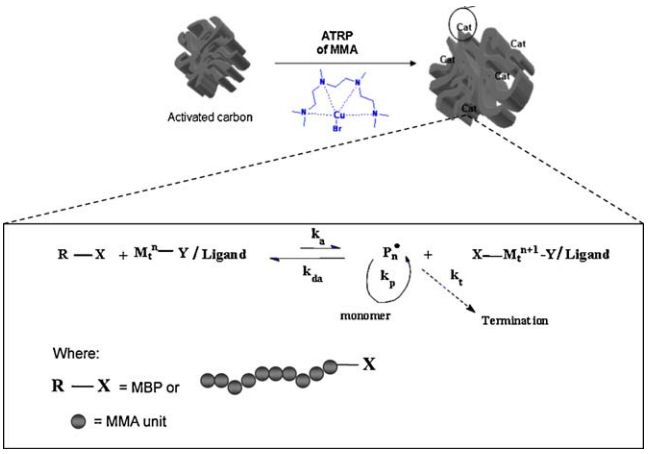

Scheme 1. Representation of CuBr/HMTETA supported on activated carbon.

3.2. Heterogeneous polymerization of MMA using active carbon as support for CuBr/HMTETA catalyst

The solid CuBr/HMTETA catalyst used for the heterogeneous polymerization of methyl methacrylate was supported on the three characterized activated carbons (Scheme 1). Table 2 shows data obtained on the polymerization reaction using the fresh catalyst and two ulterior uses of it. The copper complex supported on the active carbons seemed to be effective in controlling the polymerization reaction. Supported CuBr/HMTETA catalysts were reused in a second and a third polymerization reaction without any regeneration procedure in order to demonstrate that they are still active after a polymerization process. Leaching of catalyst once the polymerization reaction was over was detected in all cases.

CuBr/HMTETA catalyst supported on the highly microporous spherical carbon produced conversions (determined after 24 h reaction) of 70% (first use of catalyst), 63% (second use of catalyst) and 66% (third use of catalyst) (Table 2, Fig. 2a). A slow polymerization rate was obtained in the first catalyst use, but the polymerization rate increased with catalyst recycling as shown by the increase of the slope of the curve percentage of conversion

Table 2
Polymerization results.

Support	Time (h)	Conversion (%)	M_n^{exp} ($g\,mol^{-1}$)	M_n^{theor} ($g\,mol^{-1}$)	M_w/M_n	R_{Cu} (ppm)
Spherical carbon						
First use	24	70	14 938	7000	1.25	2
Second use	24	63	10 982	6300	1.25	4
Third use	24	66	12 368	6600	1.30	5
RGC-30						
First use	24	72	12 652	7200	1.13	45
Second use	24	83	12 912	8300	1.14	47
Third use	24	75	12 298	7500	1.09	44
LMA F-12						
First use	12	83	10 026	8300	1.26	73
Second use	12	75	12 549	7500	1.29	126

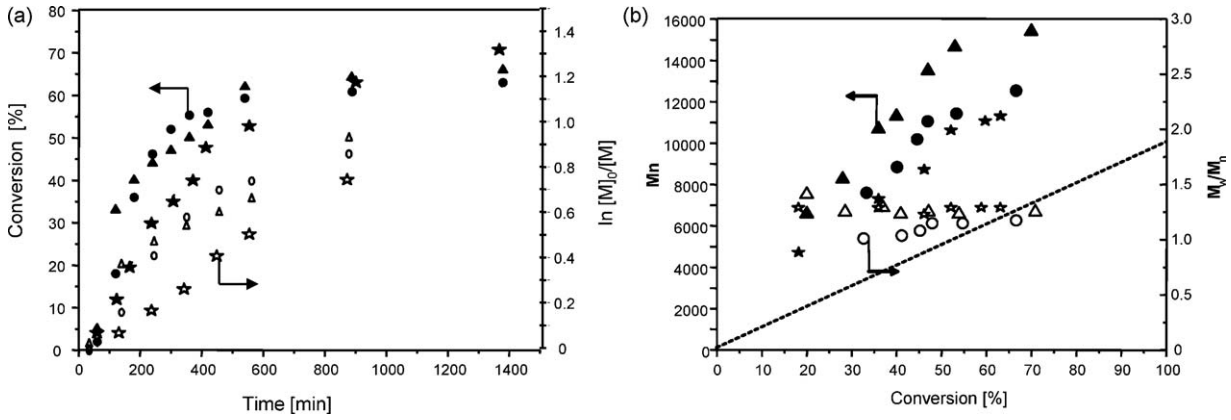

Fig. 2. (a) Kinetic plots and (b) M_n and PDI (M_w/M_n) vs. MMA conversion (%) plots in experiments for heterogeneous polymerizations in toluene with CuBr/HMTETA supported in spherical carbon (first use (★ and ☆), second use (● and ○) and third use (▲ and △) of catalyst). Theoretical M_n curve (- - -). Polymerization conditions: [MMA]/[Cu]/[MBP] = 100/1/1 in 25 vol% MMA in toluene at 85 °C.

vs. time (Fig. 2a, left). The lineal increase of the logarithm of the initial concentration of monomer (methyl methacrylate), $[M]_0$, and the concentration of monomer at a given time, [M], vs. polymerization reaction time (Fig. 2a, right) indicates that there is a constant concentration of active species in the polymerization reaction, which is consistent with a first-order kinetics with respect to the monomer. However, since termination occurs continuously, the concentration of the $Cu^{(II)}$ species in the catalyst increases and deviation from linearity may be observed, especially at high conversion percentage [39]. The reaction proceeded faster during the third use of the catalyst. Although a slower polymerization rate was obtained during the first use of the catalyst compared to that obtained with the recycled catalyst, the polydispersity index, that is, the ratio between the weight-average and the number-average molecular weights (M_w/M_n), was almost constant (around 1.3) during all catalyst uses (Fig. 2b, right, Table 2) and within the range considered for a relatively narrow molecular weight distribution ($1.0 < M_w/M_n < 1.5$), although in a well-controlled polymerization, M_w/M_n is usually less than 1.1 [40]. In all cases, the experimental molecular weight (M_n^{exp}) was higher than the theoretical molecular weight (M_n^{theor}) (Table 2), but a lineal increase of molecular weight with the increase of the conversion percentage (Fig. 2b, left) is obtained. The plots of M_n vs. conversion (Fig. 2b, left) were always linear and relatively parallel to the theoretical M_n line (represented by the dashed line in Fig. 2b), as expected [41].

When the CuBr/HMTETA catalyst was supported on the highly mesoporous LMA F-12 carbon, 83% (first catalyst use) and 75% (second catalyst use) conversions were obtained. Conversions were measured after 12 h reaction (instead of after 24 h reaction, which was the time considered for the other two activated carbons) due to the lower mechanical properties of the LMA F-12 carbon, which did not permit an extended use of the catalyst. Fig. 3a shows a decrease of conversion during the second use of the catalyst with respect to its first use. After the second use, catalyst was mechanically damaged (activated carbon powdered during reaction) and no recycling was possible afterwards. The polydispersity index of PMMA (Fig. 3b) obtained by polymerization of MMA with CuBr/HMTETA supported on the highly mesoporous LMA F-12 carbon was similar to that obtained with the microporous spherical carbon.

When CuBr/HMTETA catalyst was supported on the micro + - mesoporous RGC-30 carbon, conversions of 72% (first catalyst use), 83% (second catalyst use) and 75% (third catalyst use) were obtained 24 h after the beginning of the methyl methacrylate polymerization reaction (Table 2). Fig. 4a shows that with the RGC-30 carbon as a support a first-order kinetics is also obtained up to 600 min polymerization reaction time. The use of this micro + mesoporous carbon allowed a better control of the polymerization reaction. Thus, a narrow polydispersity index was achieved (M_w/M_n = 1.09–1.14) (Fig. 4b, right and Table 2). Besides, poly(methyl methacrylate) obtained with CuBr/HMTETA catalyst supported on the micro + mesoporous RGC-30 carbon had a weight molecular number closer to the theoretical calculated weight molecular number (dashed line in Fig. 4b).

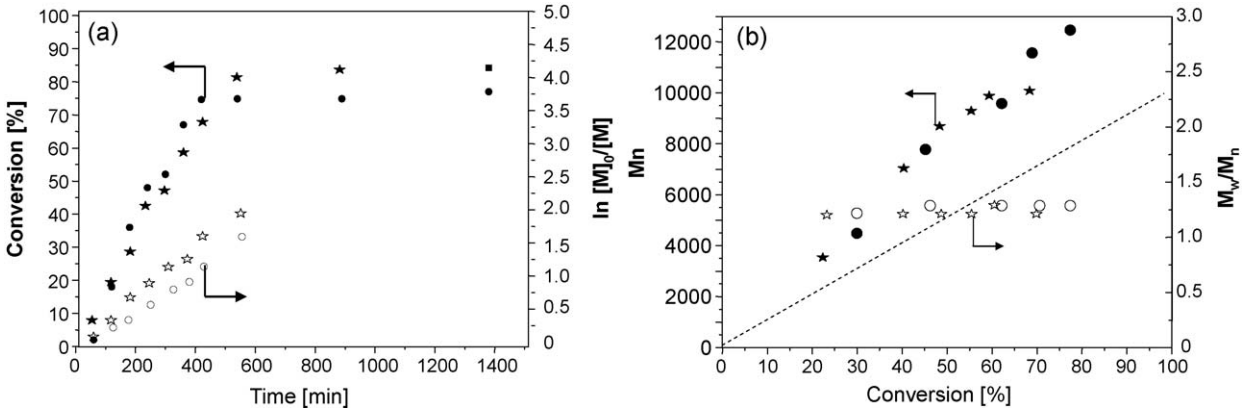

Fig. 3. (a) Kinetic plots and (b) M_n and PDI (M_w/M_n) vs. MMA conversion (%) plots in experiments for heterogeneous polymerizations in toluene with CuBr/HMTETA supported in LMA F-12 carbon (first use (★ and ☆) and second use (● and ○) of catalyst). Theoretical M_n curve (- - -). Polymerization conditions: [MMA]/[Cu]/[MBP] = 100/1/1 in 25 vol% MMA in toluene at 85 °C.

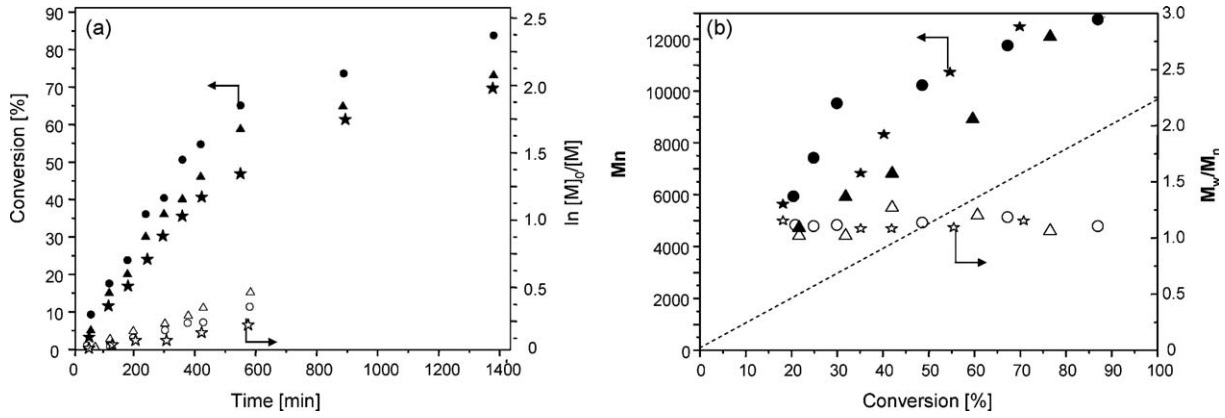

Fig. 4. (a) Kinetic plots and (b) M_n and PDI (M_w/M_n) vs. MMA conversion (%) plots in experiments for heterogeneous polymerizations in toluene with CuBr/HMTETA supported in RGC-30 carbon (first use (★ and ☆), second use (● and ○) and third use (▲ and △) of catalyst). Theoretical M_n curve (- - -). Polymerization conditions: [MMA]/[Cu]/[MBP]=100/1/1 in 25 vol% MMA in toluene at 85 °C.

CuBr/HMTETA catalyst supported on the three different activated carbons showed an adequate control of the polymerization reaction: the polydispersity index always fell in the range 1.1–1.3. However, the carbon porosity affected the control of the polymerization reaction as catalyst accessibility to the support surface may be limited by the pore size as well as by the size of the growing polymer chains [30]. Thus, the highly microporous carbon (spherical) and the mesoporous carbon (LMA F-12) were not as effective as the carbon which had micro- and mesoporosity (RGC-30). The narrowest polydispersity index (1.09) was obtained during the third use of the catalyst supported on RGC-30 carbon (Table 2). This carbon also provided a polymer with an experimental molecular weight (M_n^{exp}) closer to the theoretical molecular weight (M_n^{theor}).

Transport limitations inside micropores result in a decrease of polymerization rate, as observed when the highly microporous carbon (spherical) was used as catalyst support. However, polymerization rate increased when the CuBr/HMTETA catalyst was supported on the mesoporous carbon (LMA F-12), as deduced from the increase of the slope of the conversion vs. time curve (Figs. 2a and 3a). This reveals the importance of the accessibility of the polymer growing chains during the polymerization reaction towards the metallic complex used as a catalyst. When the LMA F-12 carbon, which exhibits mesoporosity, was used as support, the growing polymer chains easily accessed the oxidized form of the metallic complex ($Cu^{(II)}Br_2$/HMTETA), which then go back to its deactivated state ($Cu^{(I)}$Br/HMTETA) as shown in Scheme 2. These activation/deactivation reactions are critical to obtain a controlled polymerization. In absence of any side reactions other than radical termination by coupling or disproportionation, the magnitude of the equilibrium constant ($K_{eq} = k_a/k_{da}$) determines the polymerization rate. ATRP will not occur, or occur very slowly, if the equilibrium constant is too small. If the equilibrium constant is too large, a large amount of termination due to high radical concentration together with a large amount of deactivating higher oxidation state metal ($Cu^{(II)}$ in this case), will shift the equilibrium towards dormant species and may result in an apparently slower polymerization reaction [42]. Therefore, the concentration of propagating radicals and the rate of radical deactivation must be adjusted in order to achieve polymerization control. Since ATRP is a

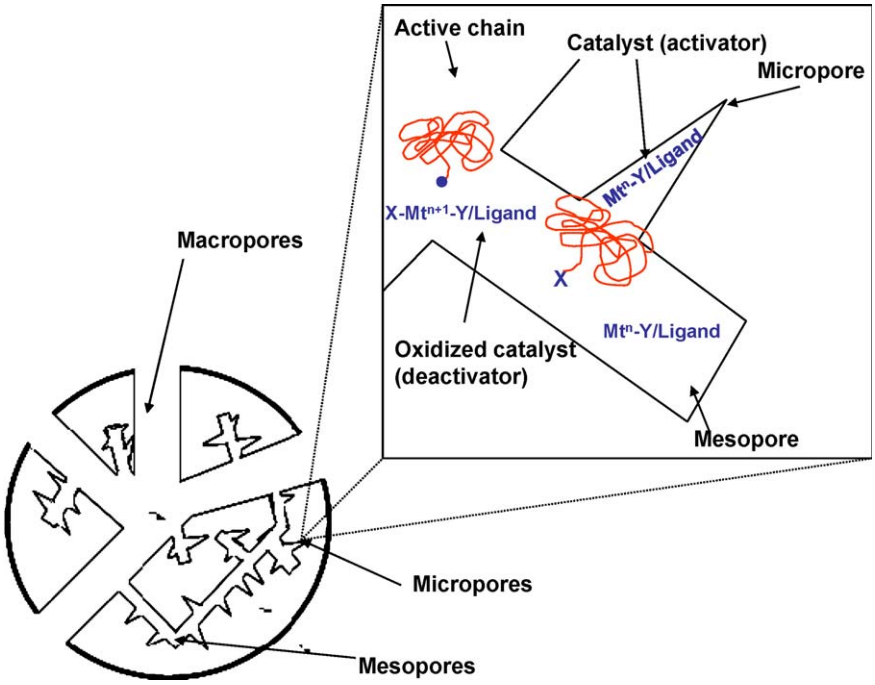

Scheme 2. Effect of pore size of activated carbon in ATRP.

catalytic process, the overall position of the equilibrium depends on the radical species ($P_n^{\bullet}$), which is the growing poly(methyl methacrylate) chain in this case, and the dormant species (alkyl halide, R–X) and the amount and reactivity of the transition metal catalyst M_t^n–Y/ligand, which is CuBr/HMTETA in this study.

The mesoporosity of the activated carbons used as support of the CuBr/HMTETA catalyst enhances the activation/deactivation process, as it allows the polymeric chains to bond to the catalyst complex, which undergoes a one-electron oxidation producing $Cu^{(II)}Br$/HMTETA (M_t^n–Y/ligand in Scheme 1) and then deactivates returning to $Cu^{(I)}Br_2$/HMTETA (X–M_t^{n+1}–Y/ligand in Scheme 1). However, in the micropores the catalyst is isolated from the growing polymeric chains located in the mesopores, or it could also be blocked in the micropores themselves when is bonded to an incipient growing polymeric chain whose size would allow it to enter a micropore. Therefore, no noticeable influence in the activation of polymeric chains is produced (Scheme 2). Consequently, porosity of activated carbon affects polymerization rate of methyl methacrylate catalyzed by CuBr/HMTETA supported on activated carbon.

When a homogeneous catalytic system is used, the atom transfer equilibrium is displaced towards the deactivated complex and, in this way a faster deactivation and a slower propagating rate are produced. Thus, control of the process is enhanced and narrower polydispersities are obtained compared to the heterogeneous catalyzed ATRP [30]. In general, polymers with considerably high polydispersities ($M_w/M_n > 1.5$) are reported using solid supported catalysts. This has been explained by slow deactivation of the growing radicals resulting form slow diffusion towards the metal centre of the catalyst complex.

However, in this study polydispersity indexes equal or below 1.3 (Table 2) were obtained when the CuBr/HMTETA catalyst was physically adsorbed on activated carbon, and a controlled polymerization of methacrylate was achieved. The most efficiently controlled polymerization (polydispersities lower than 1.15) was produced using a micro + mesoporous carbon (RGC-30) which permitted to reach a balance between activation and deactivation processes. In the microporous carbon (spherical), the narrow micropores difficulted deactivation and created an isolated reaction ambient. When the pore size is increased in RGC-30 (micro + mesoporous) and LMA F-12 (mesoporous) carbons, polymerization rate is increased. LMA F-12 carbon, with considerably high mesoporous content, enhances the polymerization rate but, at the same time, control of the polymerization reaction is not as effective. Thus, higher polydispersities are obtained compared to RGC-30 carbon. This is consistent with a favoured activation process but an inefficient deactivation process in the mesopores, which results in an increase of polymerization rate but in a lost of control over the polymerization reaction, *i.e.* polydispersities over 1.25 are obtained with LMA F-12 carbon.

One of the challenges of ATRP process is the removal and recycling of the catalyst. However, this implies the development of efficient methods of catalyst removal. Another possibility would be to continuously increase the activity of the catalytic system by reducing the amount of catalyst to a level that may be left in the final polymer. Honigfort and Brittain [23] reported that approximately 5–7% of original copper used as catalyst for ATRP remains in the final polymer. Shen et al. [24–26] detected a residual copper content below 33.4 ppm in their final polymers. Matyjaszewski et al. [18,19] published a residual copper content below 107 ppm in their system based on CuBr/bipyridine.

The CuBr/HMTETA catalyst used in this study exhibited copper leaching during the polymerization process, irrespective of the activated carbon used as catalyst support. A possible cause of leaching may be structural rearrangements of the surface copper species during reaction. The structural changes required upon copper oxidation create unstable species that favour leaching [43]. The residual copper content in the poly(methyl methacrylate) final polymer (R_{Cu}) (Table 2) was measured using inductively coupled plasma atomic emission spectroscopy (ICP-OES). The theoretical copper content, assuming that all the copper in the catalyst suffers leaching and that a 100% conversion of methyl methacrylate into poly(methyl methacrylate) is reached, would be 1329 ppm. When micro + mesoporous RGC-30 carbon was used as support of the copper catalyst, the residual copper content (R_{Cu}) was always lower than 50 ppm. However, the use of a mechanically weaker catalyst support (LMA F-12 carbon), which may be damaged during the second use of the catalyst, gave rise to a noticeable higher residual copper content in the polymer ($R_{Cu} > 100$ ppm). On the other hand, the microporous structure of spherical carbon is consistent with a low polymerization rate and, consequently, with a low residual copper. CuBr/HMTETA catalyst bonded to the growing polymer chains during polymerization reaction is blocked inside the micropores. Thus, copper leaching is reduced (Scheme 2).

All the heterogeneous polymerizations using activated carbon as support behaved kinetically similarly to several previously reported ATRP systems [11,12,15,24,30]. Although many of those catalysts are recyclable, significant losses, often up to 50%, in catalyst activity after recycling are reported. For instance, in the ATRP of methyl methacrylate (MMA) with HMTETA/CuBr physically adsorbed onto silica gel, losses in catalyst activity of 20% (between the first and second run) and 35% (between second and third runs) have been reported [15]. Faucher [44] investigated silica gel as support and ascribed the loss of activity upon recycling the supported catalyst to the presence of unsupported active-catalyst sites in solution. However, in the present study, where activated carbon has been used as a catalyst support, losses in activity remained below 10%.

On the other hand, homogeneous catalyzed ATRP of MMA using CuBr/HMTETA in toluene proceeded in a well-controlled manner and 90% conversion was achieved [37]. Conversion obtained with CuBr/HMTETA supported on halloysite nanotubes is comparable to the homogeneous catalyst. This has been attributed [37] to the fact that halloysite nanotubes have a promoting effect on the MMA polymerization rate due to the coordination of nanoclay to the carbonyl group of the monomer. When this same catalyst is supported on activated carbon a considerable high (80%) conversion is achieved, but in this case, no probable promoting effect of the support during the polymerization might be taking place, so only the influence of activated carbon textural properties has been considered.

4. Conclusions

From the above results it can be concluded that activated carbon is a suitable support of CuBr/HMTETA for ATRP of methyl methacrylate. The texture of the activated carbon plays an important role in the polymerization rate and the control of polymerization reaction, evaluated by the polydispersity index of the final poly(methyl methacrylate). The accessibility of the catalyst to pores in the activated carbon is limited by pore size and growing polymer size. Thus, transport limitations inside micropores result in a low polymerization rate. In mesopores, the access of growing polymer chains is favoured and deactivation process is enhanced. The balance between activation and deactivation processes involving $Cu^{(I)}$ and $Cu^{(II)}$ catalytic species in the kinetics of the methyl methacrylate polymerization reaction is successfully achieved when an activated carbon exhibiting both micro- and mesoporosity was used (RGC-30 carbon). Consequently, copper leaching is reduced and molecular weight control is achieved when RGC-30 carbon is used as support of CuBr/

HMTETA catalyst for the controlled polymerization of methyl methacrylate.

Acknowledgements

The Mexican Council of Science and Technology (CONACYT) is gratefully acknowledged for the Pre-Doctoral fellowship no. 187157 to S. Barrientos-Ramírez. Financial support from Conselleria d'Educació (Generalitat Valenciana, Project ACOMP2007/049) is gratefully acknowledged. We thank M. Dolores Baeza for her help with GPC experiments.

References

[1] F. Rodriguez-Reinoso, Carbon 36 (1998) 159.
[2] H. Marsh, F. Rodríguez-Reinoso, Activated Carbon, Elsevier, Oxford, 2006.
[3] F. Rodríguez-Reinoso, A. Linares-Solano, in: P.A. Thrower (Ed.), Chemistry and Physics of Carbon, vol. 21, Marcel Dekker, Inc., New York, 1989.
[4] S. Smisek, M. Cerny, Active Carbon Manufacture: Properties and Applications, Elsevier, New York, 1970.
[5] S. Urbonaite, J.M. Juárez-Galán, J. Leis, F. Rodríguez-Reinoso, G. Svensson, Microporous Mesoporous Mater. 113 (2008) 14.
[6] R.V.R.A. Rios, J. Silvestre-Albero, A. Sepúlveda-Escribano, F. Rodríguez-Reinoso, Colloids Surf. A 300 (2008) 180.
[7] J López-González, F. Martínez-Vilchez, F. Rodríguez-Reinoso, Carbon 18 (1980) 413.
[8] G. Keller, Chem. Eng. Prog. 91 (1995) 56.
[9] K. Matyjaszewski, J. Xia, Chem. Rev. 101 (2001) 2921.
[10] W. Jakubowski, N.V. Tsarevsky, T. Higashihara, R. Faust, K. Matyjaszewski, Macromolecules 41 (2008) 2318.
[11] Y. Shen, S. Zhu, R. Pelton, Macromolecules 34 (2001) 5812.
[12] G. Kickelbick, H.J. Paik, K. Matyjaszewski, Macromolecules 32 (1999) 2941.
[13] T. Otsu, T. Tazaki, M. Yoshioka, Chem. Express 5 (1990) 801.
[14] D.M. Haddleton, D. Kukulj, A.P. Radigue, Chem. Commun. (1999) 99.
[15] Y. Shen, S. Zhu, R. Pelton, Macromolecules 33 (2000) 5427.
[16] T. Liu, S. Jia, T. Kowalewski, K. Matyjaszewski, R. Casado-Portilla, J. Belmont, Langmuir 19 (2003) 6342.
[17] T. Liu, R. Casado-Portilla, J. Belmont, K. Matyjaszewski, J. Polym. Sci. Part A: Polym. Chem. 43 (2005) 4695.
[18] S.C. Hong, K. Matyjaszewski, Macromolecules 35 (2002) 7592.
[19] S.C. Hong, H.J. Paik, K. Matyjaszewski, Macromolecules 34 (2001) 5099.
[20] D.M. Haddleton, C. Waterson, P.J. Derrick, C. Jasieczek, A.J. Shooter, Chem. Commun. (1997) 683.
[21] D.M. Haddleton, D.J. Duncalf, D. Kukulj, A.P. Radigue, Macromolecules 32 (1999) 4769.
[22] S. Liou, J.T. Rademacher, D. Malaba, M.E. Pallack, W.J. Brittain, Macromolecules 33 (2000) 4295.
[23] M.E. Honigfort, W.J. Brittain, Macromolecules 36 (2003) 3111.
[24] Y. Shen, S. Zhu, F. Zeng, R. Pelton, J. Polym. Sci. Part A: Polym. Chem. 39 (2001) 1051.
[25] Y. Shen, S. Zhu, F. Zeng, R. Pelton, Macromol. Chem. Phys. 201 (2000) 1387.
[26] Y. Shen, S. Zhu, R. Pelton, Macromolecules 34 (2001) 3182.
[27] Y. Shen, S. Zhu, Macromolecules 34 (2001) 8603.
[28] Y. Shen, S. Zhu, R. Pelton, Macromol. Rapid Commun. 21 (2000) 956.
[29] T. Opstal, K. Melis, F. Verpoort, Catal. Lett. 74 (2001) 155.
[30] J.V. Nguyen, C.W. Jones, J. Polym. Sci. Part A: Polym. Chem. 42 (2004) 1384.
[31] F. Rodríguez-Reinoso, J. López-Gonzalez, C. Berenguer, Carbon 20 (1982) 185.
[32] R. Ríos, J. Silvestre-Albero, A. Sepúlveda-Escribano, M. Molina-Sabio, F. Rodríguez-Reinoso, J. Phys. Chem. C 111 (2007) 3803.
[33] J.W. Patrick, Porosity in Carbons: Characterization and Applications, Edward Arnold, London, 1995.
[34] D.H. Everett, J.C. Powl, J. Chem. Soc., Faraday Trans. 1 72 (1976) 619.
[35] D. Lozano-Castello, D. Cazorla-Amoros, A. Linares-Solano, Carbon 42 (2004) 1233.
[36] M.M. Dubinin, in: P.L. Walker (Ed.), Chemistry and Physics of Carbon, vol. 2, Dekker, New York, 1966.
[37] S. Barrientos-Ramírez, E.V. Ramos-Fernández, J. Silvestre-Albero, A. Sepúlveda-Escribano, M.M. Pastor-Blas, A. González-Montiel, Microporous Mesoporous Mater. 120 (2009) 132.
[38] K.S.W. Sing, Chem. Ind. (1968) 1520.
[39] K. Matyjaszewski, A. Kumar-Nanda, W. Tang, Macromolecules 38 (2005) 2015.
[40] T.E. Patten, K. Matyjaszewski, Adv. Mater. 10 (1998) 901.
[41] T. Pintauer, V. Coessens, K. Matyjaszewski, Prog. Polym. Sci. 26 (2001) 337.
[42] J. Queffelec, S.G. Gaynor, K. Matyjaszewski, Macromolecules 33 (2000) 8629.
[43] J.V. Nguyen, C.W. Jones, J. Polym. Sci. Part A: Polym. Chem. 42 (2004) 1367.
[44] S. Faucher, S. Zhu, Macromol. Rapid Commun. 25 (2004) 991.